Revealing true coupling strengths in two-dimensional spectroscopy with sparsity-based signal recovery

Hadas Frostig[1], Tim Bayer[1], Yonina C. Eldar[2], and Yaron Silberberg[1]

[1]Department of Physics of Complex Systems, Weizmann Institute of Science, Rehovot 76100, Israel.
[2]Department of Electrical Engineering, Technion, Haifa 32000, Israel.

June 26, 2017

Two-dimensional (2D) spectroscopy is used to study interactions between energy levels, both in the field of optics and in NMR. Conventionally, the strength of interaction between two levels is inferred from the value of their common off-diagonal peak in the 2D spectrum, termed cross peak. Yet the stronger diagonal peaks often have long tails that extend into the locations of the cross peaks and alter their values. Here we introduce a method for retrieving the true interaction strengths using sparse signal recovery techniques, and apply our method in 2D Raman spectroscopy experiments.

Keywords: multidimensional spectroscopy; sparsity-based algorithms; nonlinear optics;

INTRODUCTION

Quantifying coupling between energy levels is key to retrieving information about the structure of a molecule and its interaction with the environment. The coupling can be studied using two-dimensional (2D) spectroscopy, where the system is excited via one energy level, and probed via another, giving information about the energy transfer between the two. Since excitation and probing directly in the frequency domain would require multiple sources that are both in the correct frequency range to excite these transitions and have some spectral tunability, this approach is technically challenging. Alternatively, the excitation and probing can be done in the time domain, using short pulses. The data may then be Fourier-transformed to retrieve the spectral response. Information about the coupling between two energy levels, ω_α and ω_β, is extracted from the magnitude of their cross-peak in the 2D spectral response, at coordinates $(\omega_\alpha, \omega_\beta)$.[1] This technique, termed two-dimensional Fourier-Transform (2D-FT)spectroscopy, is widely used and applied in two-dimensional optical spectroscopies (2D-Vis, 2D-IR, and 2D Raman),[1–9] as well as in two-dimensional nuclear magnetic resonance spectroscopy (2D-NMR).[10–12]

Though the discrete Fourier transform, often realized by the fast Fourier transform (FFT) algorithm, is a powerful tool for spectral analysis, it can be limiting in cases where the time-domain signal is comprised of several independent components. In the spectra of such signals, the value at a particular frequency is in fact the coherent sum of the spectral responses of all time-domain signal components at that frequency. Since the majority of signals are comprised of spectral components that are not infinitely narrow, the tails of the stronger signal components may spill into, or even cover, other weaker features. This effect is particularly problematic when examining cross peaks in a 2D spectrum, which are by nature weaker than their corresponding diagonal peaks.

Here we present a signal analysis method based on sparse signal recovery which eliminates such ambiguities, by identifying each component of the time-domain signal and finding its own spectral response. Our method applies the Block Orthogonal Matching Pursuit (BOMP) algorithm by Eldar *et al.*[13] directly to the 2D time-domain data. Using BOMP, the stronger signal components that cause diagonal peaks are first identified and removed and then the weaker cross-peak signal is analyzed.

To demonstrate the difficulties that arise in cross-peak analysis using FFT and their possible resolution, we will discuss an example from 2D Raman spectroscopy.[8] A typical pulse sequence used for impulsive excitation in 2D Raman spectroscopy is shown in the inset of Fig. 1a. The two time delays, $t^{(1)}$ and $t^{(2)}$, are scanned and the signal is measured for each delay pair (the analysis of time-resolved 2D spectra is discussed at the end of the following section). Fig. 1a shows the results of a simulation of 2D Raman spectroscopy performed on CCl_4 molecules, in which the coupling between energy levels was turned *off* (See SI II for details). The corre-

sponding 2D spectrum, computed by applying FFT to the data in Fig. 1a, is shown in Fig. 1b. The reflected second quadrant is presented for clarity, due to artifacts on the diagonal of the first quadrant. The peaks on the diagonal (dashed black line) correspond to the three Raman lines of CCl_4, namely 217, 313 and 459cm^{-1}. Though no cross peaks should be present, the long tail from the diagonal 313cm^{-1} peak combines with the tail from the diagonal 459cm^{-1} peak to form a false peak at (313cm^{-1},459cm^{-1}) (marked by a red arrow). Such long tails can be caused by two mechanisms: physical broadening of the vibrational level, and artifacts due to the discrete nature of FFT. The former mechanism, homogenous broadening, creates long decaying tails due to the Lorentzian function in the molecular lineshape. The latter mechanism is known as *spectral leakage*, and is a result of the convolution of the true spectral response with a *sinc* function due to the finite temporal window of the measurement. A partial solution for spectral leakage is provided by apodization, yet at the expense of a loss in both resolution and sensitivity.[14,15]

In addition to the problems caused by the long tails, off-diagonal peaks between each molecular frequency and its overtones add additional strong features to the 2D spectrum that may interfere with reading the cross-peak values. These overtone peaks can be caused both by impulsive excitation of a single level and by multiple excitations, and are present in all Fourier-transform 2D spectroscopy methods (see below). An example of this difficulty can be seen in Fig. 1b as well. An off-diagonal peak at (217cm^{-1},434cm^{-1}), between the 217cm^{-1} line and its first overtone, covers the location of another potential cross peak, at (217cm^{-1},459cm^{-1}) (marked by a brown arrow).

In this work, the BOMP algorithm is used to separate the spectral responses of these signal components from one another, using prior knowledge about the signal form. Indeed, compressed sensing (CS),[16,17] which also makes use of sparse signal recovery techniques, was introduced in recent years as a means of accelerating 2D-FT experiments by reducing the number of measurements needed, or equivalently, super-resolving the acquired data in the spectral domain.[18–29] Yet the aims of our BOMP analysis and CS are fundamentally different. While BOMP analysis is used here to fit the signal to a model, CS is typically used to approximately reconstruct the 2D spectrum that would be obtained using FFT, but with a shorter acquisition time. Therefore, CS cannot separate signal components that inherently overlap in the frequency domain, even given unlimited spectral resolution (for example due to homogenous broadening).

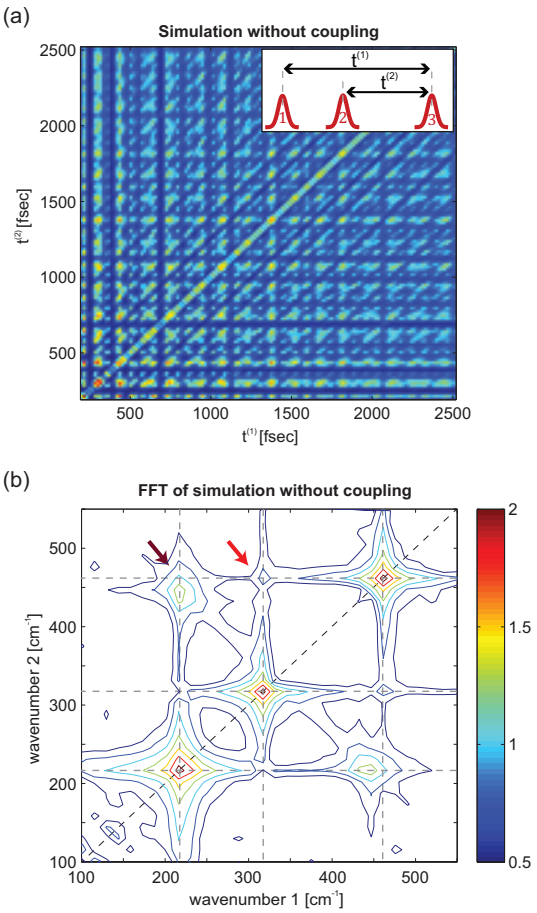

Figure 1: Simulation: an example of difficulties in interpreting 2D-FT spectra. (a) The simulated 2D Raman spectroscopy time-domain data of molecules in which the coupling between vibrational levels was turned *off*. Inset: A typical three pulse sequence used in 2D Raman spectroscopy measurements (b) The corresponding 2D spectrum, computed with FFT. The arrows mark false features that appear as cross peaks, though no cross peaks should be present. The plot is presented in log scale.

MATERIALS AND METHODS

BOMP is an efficient method for recovery of block-sparse signals. Whereas a signal is considered sparse if it can be represented in some basis where most of the coefficients of the basis vectors are zero, a signal is considered block-sparse when these nonzero coefficients represent groups of vectors.[30] For example, a 1D spectrum is sparse if the number of principle molecular frequencies it contains is small relative to the spectral window, and is block-sparse if each such principle frequency predicts the appearance of several related frequencies in the spectrum, such as its overtones. 2D spectroscopy data is a natural candidate for reconstruction with BOMP, since its spectral response is highly clustered. To understand why, let us consider the form of the acquired data. In a 2D spectroscopy experiment, the delays $t^{(1)}$ and $t^{(2)}$ in the three pulse sequence become discrete vectors of equally spaced measurement points, $t^{(1)} = t_1^{(1)}, t_2^{(1)}, ...t_i^{(1)}$ and $t^{(2)} = t_1^{(2)}, t_2^{(2)}, ...t_j^{(2)}$, and therefore the measured data forms a 2D matrix, as in Fig. 1a. For a sample with a single energy level ω, a typical matrix element of the experimental data set will have the form:

$$S_{ij}\left(\omega;t_i^{(1)},t_j^{(2)}\right)= \quad (1)$$
$$\sum_{n=0}^{N}\sum_{m=0}^{N}A_{nm}D\left(n\omega,\phi_n,\sigma_n,\gamma_n;t_i^{(1)}\right)\times$$
$$D\left(m\omega,\phi_m,\sigma_m,\gamma_m;t_j^{(2)}\right)+$$
$$\sum_{k=0}^{N}\sum_{l=0}^{N}D\left(k\omega,\phi_k,\sigma_k,\gamma_k;|t_i^{(1)}-t_j^{(2)}|\right)\times$$
$$\left[B_{kl}D\left(l\omega,\phi_l,\sigma_l,\gamma_l;t_i^{(1)}\right)+C_{kl}D\left(l\omega,\phi_l,\sigma_l,\gamma_l;t_j^{(2)}\right)\right]$$

where i and j are the matrix indices, $D(\omega,\phi,\sigma,\gamma;t)$ is a decaying oscillatory function of frequency ω that includes homogenous broadening of width γ and inhomogenous broadening of width σ, ϕ is the phase of the oscillations with respect to the decaying envelope, n,m,k,l represent the $n^{th},m^{th},k^{th},l^{th}$ overtone accordingly, A_{nm},B_{kl},C_{kl} are proportionality constants, and the sum is performed up to N, the highest overtone with a significant contribution to the signal. The second term of Eq. (1) appears since a pulse sequence with two time delays, $t^{(1)}$ and $t^{(2)}$, necessarily also contains their difference (see inset of Fig. 1a) and therefore also a signal component oscillating as a function of that difference. The overtones of each frequency of the sample appear whenever the time-domain oscillating signal form is more impulsive than a pure decaying cosine and when transitions due to multiple excitations are present[31] (a variable anharmonicity can be added when relevant, see SI I part 1). The 0^{th} overtone represents a DC component, i.e. a vector with decay only, and hence S_{i0} and S_{0j} appear as axial peaks in the 2D spectrum. For a sample with multiple energy levels, excluding interactions between the levels, the total sample response is $S_{ij}^{tot}=\sum_{\omega}S_{ij}(\omega)$.

As can be seen from Eq. (1), the existence of a certain molecular frequency ω_α in the sample predicts the appearance of a distinct group of terms in the signal, encompassing the diagonal ($m=n$), axial ($m=0$ or $n=0$), overtone ($m\neq n$ and $m,n\neq 0$) and time-difference terms of ω_α. This group serves as the basic block used by BOMP in the analysis in the following manner: A large database of blocks is created (termed *dictionary*) where each block represents a frequency of an energy level that could be present in the sample. The algorithm searches iteratively for the block with the maximal sum of inner products between the block members and the data. Each iteration retrieves one molecular frequency and the magnitude of all associated terms, removes these terms from the data and orthogonalizes the residual.[32] The halting condition may be a bound on the error or the number of molecular frequencies, if known. Prior knowledge of the lineshape parameters, or any unknown parameter in the model, is not required, since BOMP can be used to recover the values of those parameters in addition to the molecular frequencies (see SI I, part 1). Once BOMP has removed all the signal components associated with the stronger peaks, represented in Eq. (1), the residual data is fitted to a matrix that describes coupling between modes, with entries of the form:

$$S_{ij}^{coup}\left(\omega_\alpha,\omega_\beta;t_i^{(1)},t_j^{(2)}\right)= \quad (2)$$
$$A_o\,D\left(\omega_\alpha,\phi_\alpha,\sigma_\alpha,\gamma_\alpha;t_i^{(1)}\right)D\left(\omega_\beta,\phi_\beta,\sigma_\beta,\gamma_\beta;t_j^{(2)}\right)+$$
$$D\left(\omega_\alpha,\phi_\alpha,\sigma_\alpha,\gamma_\alpha;|t_i^{(1)}-t_j^{(2)}|\right)\times$$
$$\left[B_oD\left(\omega_\beta,\phi_\beta,\sigma_\beta,\gamma_\beta;t_i^{(1)}\right)+C_oD\left(\omega_\beta,\phi_\beta,\sigma_\beta,\gamma_\beta;t_j^{(2)}\right)\right]$$

according to the retrieved molecular frequencies. Here $\omega_\alpha,\omega_\beta$ represent two different energy levels of the sample, and A_o,B_o,C_o are constants. This step recovers the cross-peak values and concludes the analysis.

Since BOMP fits the signal to a model, it is related to spectral analysis methods such as parametric linear prediction techniques, filter diagonalization method, maximum likelihood, Bayesian analysis, multi-dimensional decomposition, and implementations of nonlinear least-squares fitting.[33–44] However, for sparse signals such as 2D spectroscopy data, sparse signal recovery methods have been shown to fit the signal robustly in the presence of noise and have provable recovery guarantees.[16,45] In fact, the BOMP algorithm has been shown to come close to the Cramer-Rao bound,[46] and was able to retrieve cross-peak values that were an order of magnitude weaker than the noise level in a simulation we performed (see SI 2.2). Moreover, the addition of the block-form constraint serves to reduce the parameter space of the problem. These two properties of BOMP allow for recovery of the correct signal representation in larger solution spaces than would be possible otherwise. Successful recovery with BOMP generally relies on two main criteria in the user input: a sufficient number of measured data points and the quality of the block-dictionary. For an in-depth discussion of these criteria, as well as other aspects of the performance of BOMP, see SI 2.

When analyzing time-resolved 2D spectra, the 2D spectrum for each waiting time can generally be analyzed with BOMP as currently implemented. Since BOMP extracts the magnitudes of all the peaks in an analyzed spectrum, the variations in their magnitudes as a function of waiting time are directly obtained from the results. As BOMP can be used to extract the values of other parameters, such as lineshape parameters, it can be utilized to follow their variations as a function of waiting time as well. Models that include population and coherence transfer[47–49] can be accommodated by adding cross-peaks shifted by diagonal anharmonicity and diagonal peaks shifted by off-diagonal anharmonicity. The $D(\omega,\phi,\sigma,\gamma;t)$ function used here already includes bimodal decay, yet adding a third decay rate might be necessary in some cases of population and coherence transfer as well. BOMP can be extended to analyze three-

dimensional spectra, as discussed in more detail in SI 1.

RESULTS AND DISCUSSION

Numerical results

In order to test the performance of BOMP analysis we prepared two sets of simulated 2D Raman spectroscopy data. The first set simulates a sample of CCl_4 without any coupling between vibrational levels and the second simulates a sample of CCl_4 with coupling. The sampling rate and window size were set to match those of a typical 2D Raman experiment (see SI 3 for simulation details). For comparison, both data sets were first analyzed using FFT, producing the results in Fig. 2. We can observe only minor differences between the simulation without coupling (Fig. 2a) and the simulation with coupling (Fig. 2b), since features from the diagonal peaks at 217cm^{-1} and 459cm^{-1} and from the overtone peak at (217cm^{-1},434cm^{-1}) almost entirely cover the cross-peak locations (marked with black x's).

In contrast, analyzing the same two data sets using BOMP clearly shows the differences between the sets with and without coupling. The cross-peak values retrieved using BOMP analysis on both sets (represented by A_o in Eq. 2) are presented in Fig. 3. We observe that while BOMP finds significant energy in the (217cm^{-1},459cm^{-1}) and (313cm^{-1},459cm^{-1}) cross peaks in the simulation with coupling (orange), it finds noise-level energy for the same cross peaks in the simulation without coupling (purple). Furthermore, to verify that the retrieved values of the cross peaks are correct we prepared a third simulated data set, which contains only terms that cause cross peaks and no terms that cause diagonal, axial, and overtone peaks (see SI 3). In this data set, the cross-peak values remain the same but all the tails from the diagonal and overtone peaks are absent, so FFT yields the true cross-peak values. The results from analyzing this set with FFT, shown in Fig. 3 in blue, agree nicely with the results of running BOMP on the full simulation with coupling (orange). From both tests we may conclude that BOMP analysis does in fact retrieve the true, background-free, cross-peak values. For a comparison with the results from simulated data with additive white Gaussian noise see SI 2.

Experimental results

We now turn to analyze the experimental results from a 2D Raman spectroscopy measurement on liquid CCl_4[8] with BOMP. The cross-peak values retrieved from the experimental data are shown in green in Fig. 3. The error-bar values were computed by propagating the error caused by experimental noise in the time-domain measurement (SNR of ∼10:1). These results can also be used to create a clean, high-resolution 2D spectral plot of the cross-peak signal only. The advantage of plotting the cross-peak component of the signal on its own is demonstrated in Fig. 4, which compares several analysis methods of the experimental data. The results from conventional FFT analysis, shown in Fig. 4a, display long tails extending from the diagonal peaks, as well as strong overtone peaks and additional artifacts. The plot clearly contains features covering the cross-peak locations (marked by black x's) and lacks the resolution necessary for reading off the cross-peak values. Fig. 4b shows the full 2D spectral response, including all time-domain signal components, retrieved by BOMP from the same data. The artifact on the diagonal (see SI I, Eq. 4) and features due to noise were not reconstructed for clarity. Since this plot is constructed directly in the spectral domain, it is equivalent to the spectral response that would be retrieved using FFT from a measurement with an infinitely large temporal window. Though the plot is free from spectral leakage and has significantly higher resolution, the physical properties of the signal still prevent proper cross-peak analysis. The tails caused by homogenous broadening still cover the location of the (217cm^{-1},313cm^{-1}) cross peak, and alter the shape of the (313cm^{-1},459cm^{-1}) cross peak, likely modifying its value. Moreover, the (217cm^{-1},434cm^{-1}) overtone peak interferes with the (217cm^{-1},459cm^{-1}) cross peak. Therefore, eliminating spectral leakage alone, by adding more data points or with conventional compressed sensing techniques,[24,25,27,29] would not have provided an adequate solution. It is worth noting that simply removing the real part of the lineshape (dispersive), as is done using phase-cycling[50,51] or by plotting the real part of the sum of the rephasing and non-rephasing spectra would have not been sufficient either, as the imaginary part of the homogenously-broadened lineshape (absorptive) still creates significant tails. Lastly, Fig. 4c shows the 2D spectral response corresponding to the cross-peak signal only, retrieved by BOMP. This spectrum is free from any additional components or artifacts that may distort the cross peaks, and provides a high-resolution, accurate representation of a relatively weak signal component that would be otherwise hard to study.

CONCLUSIONS

In this work, Block Orthogonal Matching Pursuit was used to analyze data from a 2D Raman spectroscopy experiment. The analysis was performed by identifying and removing the stronger signal components before analyzing the coupling signal and therefore eliminated the ambiguities in cross-peak analysis associated with the use of FFT. Since BOMP provides an approximate analytical representation of the 2D spectral response, the analysis method presented here can be used to explore properties of the signal other than the cross peaks, such as the the lineshape, phase, and magnitude of each peak in the spectrum. For highly complex spectra with non-standard features, BOMP can be used in conjunction with FFT and other tools that can assist in building the proper dictionary. Furthermore, BOMP can be combined with dictionary learning algorithms[52] so that the optimal dictionary can be learned from the data.

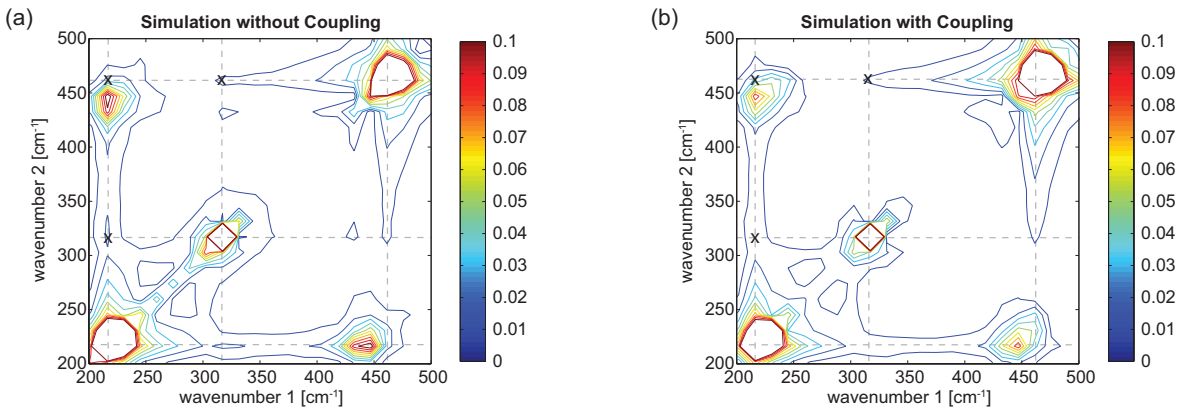

Figure 2: Analyzing simulations with and without coupling using FFT. (a) The 2D FFT of simulated 2D Raman spectroscopy data of CCl_4 without coupling. (b) The 2D FFT of simulated CCl_4 data with coupling. Both spectra are normalized. Due to the overtone peaks and the long tails of the diagonal peaks only minor differences between the two simulations are discernible, and the true values of the cross peaks in b are hard to read off (locations marked with black x's).

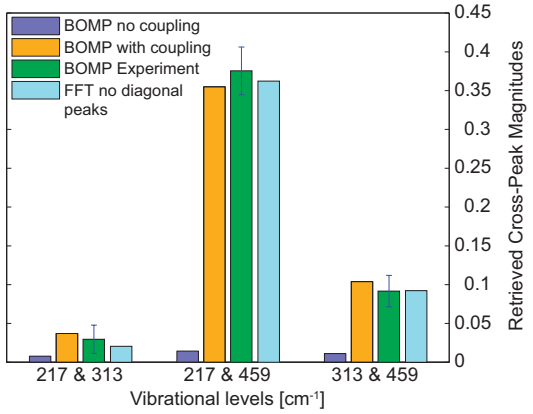

Figure 3: Analyzing the simulations presented in Fig. 2 and experimental data with BOMP. The cross-peak values retrieved by BOMP from the simulation without coupling (purple), the simulation with coupling (orange) and the experimental data (green). The cross-peak values of a simulation with coupling *only* and therefore without any tails, calculated using FFT, are presented for comparison (blue). The cross-peak values from the three data sets with coupling agree nicely.

BOMP analysis could be applicable to a wide range of Fourier-transform spectroscopies, and may allow for successful recovery of the parametric form of the acquired data where non sparsity-based techniques fail. While much work has been done in the field of multidimensional NMR with non-Fourier analysis methods for spectral analysis, there are fewer such works in multidimensional optical spectroscopy. We therefore believe that BOMP analysis may enable the study of aspects in spectral responses that would not be possible to study otherwise with optical spectroscopy.

CONFLICT OF INTEREST

The authors declare no conflict of interest.

ACKNOWLEDGEMENTS

The authors thank J. C. Hoch, N. Dudovich and L. Chuntonov for helpful discussions. This work was supported by Icore (Israeli centres of research excellence of the ISF), and the Crown Photonics Center.

Supplementary information accompanies the manuscript on the Light: Science & Applications website (http://www.nature.com/lsa/)

References

[1] Jonas DM. Two-Dimensional Femtosecond Spectroscopy. Annu Rev Phys Chem. 2003;54:425–463.

[2] Tanimura Y, Mukamel S. Two-Dimensional Femtosecond Vibrational Spectroscopy of Liquids. J Chem Phys. 1993;99:9496–9511.

[3] Tian P, Keusters D, Suzaki Y, Warren WS. Femtosecond Phase-Coherent Two-Dimensional Spectroscopy. Science. 2003;300:1553–1555.

[4] Brixner T, Stenger J, Vaswani HM, Cho M, Blankenship RE, Fleming GR. Two-Dimensional Spectroscopy of Electronic Couplings in Photosynthesis. Nature. 2005;434:625–628.

[5] Tokmakoff A, Lang MJ, Larsen DS, Fleming GR. Two-Dimensional Raman Spectroscopy of Vibrational Interactions in Liquids. Phys Rev Lett. 1997;79:2702–2705.

[6] Asplund MC, Zanni MT, Hochstrasser RM. Two-Dimensional Infrared Spectroscopy of Peptides by Phase-Controlled Femtosecond Vibrational Photon Echoes. Proc Natl Acad Sci U S A. 2000;97:8219–8224.

[7] Fayer M. Fast Protein Dynamics Probed with Infrared Vibrational Echo Experiments. Annu Rev Phys Chem. 2001;52:315–356.

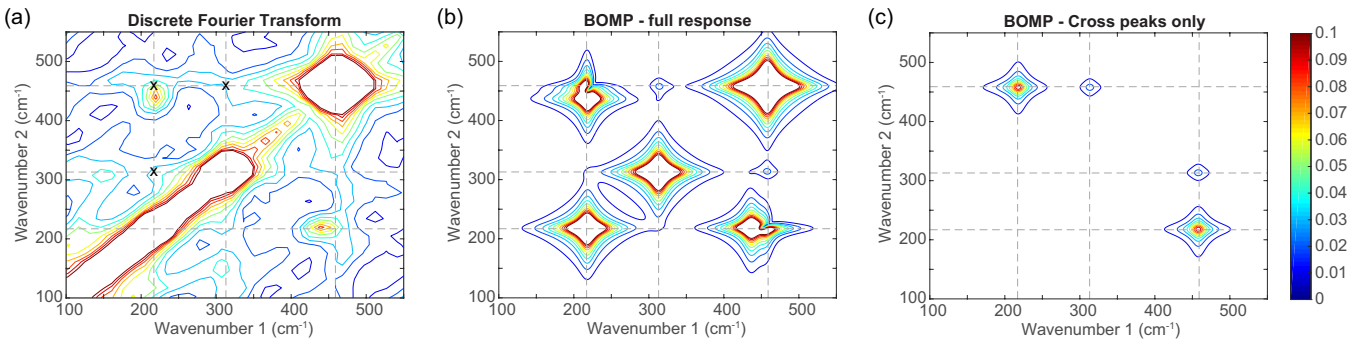

Figure 4: Experimental results: 2D Raman spectra of CCl_4, computed with FFT and BOMP. (a) The 2D spectrum computed with FFT from the measured 2D time-domain data. The cross-peak locations, which are completely covered by tails of strong features, are marked with black x's. (b) The full 2D spectrum, including all signal components, retrieved with BOMP from the measured data. This spectrum is equivalent to the spectrum that FFT would retrieve from an ideal measurement, with an infinitely-large temporal window. The cross-peak locations are still partially covered. (c) The 2D spectrum of the coupling component *only*, retrieved with BOMP from the measured data. All spectra are normalized.

[8] Frostig H, Bayer T, Dudovich N, Eldar YC, Silberberg Y. Single-Beam Spectrally Controlled Two-Dimensional Raman Spectroscopy. Nat Photonics. 2015;9:1–5.

[9] Dudovich N, Oron D, Silberberg Y. Single-Pulse Coherently Controlled Nonlinear Raman Spectroscopy and Microscopy. Nature. 2002;418:512–514.

[10] Jeener J, Meier BH, Bachmann P, Ernst RR. Investigation of Exchange Processes by Two-Dimensional NMR Spectroscopy. J Chem Phys. 1979;71:4546–4553.

[11] Englander SW, Mayne L. Using Hydrogen-Exchange Labeling and Two-Dimensional NMR. Annu Rev Biophys Biomol Struct. 1992;21:243–265.

[12] Frydman L, Blazina D. Ultrafast Two-Dimensional Nuclear Magnetic Resonance Spectroscopy of Hyperpolarized Solutions. Nat Phys. 2007;3:415–419.

[13] Eldar YC, Kuppinger P, Bolcskei H. Block-Sparse Signals: Uncertainty Relations and Efficient Recovery. IEEE Trans Signal Process. 2010;58:3042–3054.

[14] Naylor DA, Tahic MK. Apodizing Functions for Fourier Transform Spectroscopy. J Opt Soc Am A Opt Image Sci Vis. 2007;24:3644–3648.

[15] Parker SF, Patel V, Tooke PB, Williams KPJ. The Effect of Apodization and Finite Resolution on Fourier Transform Raman Spectra. Spectrochim Acta. 1991;47:1171–1178.

[16] Duarte MF, Eldar YC. Structured Compressed Sensing : From Theory to Applications. IEEE Trans Signal Process. 2011;59:4053–4085.

[17] Kutyniok G, Eldar YC. Compressed Sensing: Theory and Application. Cambridge University Press; 2012.

[18] Jaravine V, Ibraghimov I, Orekhov VY. Removal of a Time Barrier for High-Resolution Multidimensional NMR Spectroscopy. Nat Methods. 2006;3:605–607.

[19] Lustig M, Donoho D, Pauly JM. Sparse MRI: The Application of Compressed Sensing for Rapid MR Imaging. Magn Reson Med. 2007;58:1182–1195.

[20] Rovnyak D, Frueh DP, Sastry M, Sun ZYJ, Stern AS, Hoch JC, et al. Accelerated Acquisition of High Resolution Triple-Resonance Spectra Using Non-Uniform Sampling and Maximum Entropy Reconstruction. J Magn Reson. 2004;170:15–21.

[21] Coggins BE, Venters RA, Zhou P. Radial Sampling for Fast NMR: Concepts and Practices over Three Decades. Prog Nucl Magn Reson Spectrosc. 2010;57:381-419.

[22] Holland DJ, Bostock J, Gladden LF, Nietlispach D. Fast Multidimensional NMR Spectroscopy Using Compressed Sensing. Angew Chem Int Ed. 2011;50:6548-6551.

[23] Kazimierczuk K, Orekhovb V. Non-uniform sampling: post-Fourier era of NMR data collection and processing. Magn Reson Chem. 2015;53:921-926.

[24] Katz O, Levitt JM, Silberberg Y. Compressive Fourier Transfrom Spectroscopy. arXiv. 2010;(1006.2553 [physics.optics]).

[25] Sanders JN, Saikin SK, Mostame S, Andrade X, Widom JR, Marcus AH, et al. Compressed Sensing for Multidimensional Spectroscopy Experiments. J Phys Chem Lett. 2012;3:2697–2702.

[26] Mobli M, Maciejewski MW, Schuyler AD, Stern AS, Hoch JC. Sparse Sampling Methods in Multidimensional NMR. Phys Chem Chem Phys. 2012;14:10835.

[27] Almeida J, Prior J, Plenio MB. Computation of Two-Dimensional Spectra Assisted by Compressed Sampling. J Phys Chem Lett. 2012;3:2692–2696.

[28] Andrade X, Sanders JN, Aspuru-Guzik A. Application of Compressed Sensing to the Simulation of Atomic Systems. Proc Natl Acad Sci. 2012;109:13928–13933.

[29] Dunbar JA, Osborne DG, Anna JM, Kubarych KJ. Accelerated 2D-IR Using Compressed Sensing. J Phys Chem Lett. 2013;4:2489–2492.

[30] Eldar YC, Mishali M. Robust Recovery of Signals from a Structured Union of Subspaces. IEEE Trans Inf Theory. 2009;55:5302–5316.

[31] Bax A, De Jong PG, Mehlkopf AF, Smidt J. Separation of the Different Orders of NMR Multiple-Quantum Transitions by the Use of Pulsed Field Gradients. Chem Phys Lett. 1980;69:567–570.

[32] Pati YC, Rezaiifar R, Krishnaprasad PS. Orthogonal Matching Pursuit: Recursive Function Approximation with Applications to Wavelet Decomposition. Proc 27th Asilomar Conf Signals, Syst Comput. 1993;1:40–44.

[33] Schussheim AE, Cowburn D. Deconvolution of High-Resolution Two-Dimensional NMR Signals by Digital Signal Processing with Linear Predictive Singular Value Decomposition. J Magn Reson. 1987;71:371–378.

[34] Wise F, Rosker M, Millhauser G, Tang C. Application of Linear Prediction Least-Squares Fitting to Time-Resolved Optical Spectroscopy. IEEE J Quantum Electron. 1987;23:1116–1121.

[35] Zeng Y, Tang J, Bush CA, Norris JR. Enhanced Spectral Resolution in 2D NMR Signal Analysis Using Linear Prediction Extrapolation and Apodization. J Magn Reson. 1989;83:473–483.

[36] Bretthorst GL. Bayesian Analysis. I. Parameter Estimation Using Quadrature NMR Models. J Magn Reson. 1990;88:533–555.

[37] Beer RD, Ormondt DV. Analysis of NMR Data Using Time Domain Fitting Procedures Spectrum Analysis. In: In-Vivo Magn. Reson. Spectrosc. I Probeheads Radiofreq. Pulses. Springer Berlin Heidelberg; 1992. p. 201–248.

[38] Chylla RA, Markley JL. Theory and application of the maximum likelihood principle to NMR parameter estimation of multidimensional NMR data. J Biomol NMR. 1995;5:245–258.

[39] Mandelshtam V, Taylor H, Shaka A. Application of the Filter Diagonalization Method to One- and Two-Dimensional NMR Spectra. J Magn Reson. 1998;133:304–312.

[40] Massiot D, Fayon F, Capron M, King I, Le Calve S, Alonso B, et al. Modelling one- and two-dimensional solid-state NMR spectra. Magn Reson Chem. 2002;40:70-76.

[41] Orekhov VU, Jaravine VA. Analysis of non-uniformly sampled spectra with multi-dimensional decomposition. Prog Nucl Magn Reson Spectrosc. 59 (2011) 271292.

[42] Khalil M, Demirdoven N, Tokmakoff A. Coherent 2D IR Spectroscopy : Molecular Structure and Dynamics in Solution. J Phys Chem A. 2003;107:5258–5279.

[43] Stokkum IHMV, Larsen DS, Grondelle RV. Global and Target Analysis of Time-Resolved Spectra. Biochim Biophys Acta. 2004;1657:82–104.

[44] Duan Hg, Stevens AL, Nalbach P, Thorwart M, Prokhorenko VI, Miller RJD. Two-Dimensional Electronic Spectroscopy of Light-Harvesting Complex II at Ambient Temperature : A Joint Experimental and Theoretical Study. J Phys Chem A. 2015;119:12017–12027.

[45] Donoho DL, Elad M, Temlyakov V. Stable Recovery of Sparse Overcomplete Representations in the Presence of Noise. IEEE Trans Inf Theory. 2006;52:6–18.

[46] Ben-Haim Z, Eldar YC. Near-Oracle Performance of Greedy Block-Sparse Estimation Techniques From Noisy Measurements. IEEE J Sel Topics Signal Process. 2011;5:1032–1047.

[47] Piryatinski A, Chernyak V, Mukamel S. Vibrational-Exciton Relaxation Probed by Three-Pulse Echoes in Polypeptides. Chemical Physics. 2001 May;266(2–3):285–294.

[48] Khalil M, Demirdöven N, Tokmakoff A. Vibrational Coherence Transfer Characterized with Fourier-Transform 2D IR Spectroscopy. The Journal of Chemical Physics. 2004;121(1):362.

[49] Nee MJ, Baiz CR, Anna JM, McCanne R, Kubarych KJ. Multilevel Vibrational Coherence Transfer and Wavepacket Dynamics Probed with Multidimensional IR Spectroscopy. The Journal of Chemical Physics. 2008;129(8):084503.

[50] Bax A, Mehlkopf AF, Smidt J. Absorption Spectra from Phase-Modulated Spin Echoes. J Magn Reson. 1979;35:373–377.

[51] Khalil M, Demirdöven N, Tokmakoff A. Obtaining Absorptive Line Shapes in Two-Dimensional Infrared Vibrational Correlation Spectra. Phys Rev Lett. 2003;90(4):047401.

[52] Zelnik-Manor L, Rosenblum K, Eldar YC. Dictionary Optimization for Block-Sparse Representations. IEEE Trans Signal Process. 2012;60:2386–2395.